Ultra Long Orbital Tethers Behave Highly Non-Keplerian and Unstable

RADU D. RUGESCU[1], DANIELE MORTARI[2]
[1]Fulbright Senior Researcher, Texas A&M Univ., USA, rugescu@yahoo.com
[2]Assoc. Professor, Texas A&M University, www.aero.tamu.edu, mortari@tamu.edu,
701A HR Bright Building, 3141 TAMU, College Station, Texas, USA,

Abstract: - Large twin tethers are investigated as possible competitive-cost tools for non-gasdynamic descent, landing, takeoff and return from target celestial bodies and as passive tools for debris retrieval from orbit. The particular behavior of orbiting bodies connected with long cables is a recent preoccupation in astrodynamics and proves being full of unexpected results. The investigation here presented is focused on the non-Keplerian behavior of such large tether systems, considered in a first approximation as rigid or very stiff and massless. The investigation starts with the feasibility of non-gasdynamic orbital deployment of twin tethers without any involvement of expensive rocket propulsion means. The free tether release systems are associated to a horizontal impulsive separation (HIS) and eventual friction-free deployment to the desired length. This horizontal deployment seems to supply the most productive means of continuous separation and departure of masses in orbit. The relative motion during separation is studied and the observation is made that a considerable kinetic moment of the system preserves during all eventual phases of the flight. After the friction-free deployment the extending cable is instantly immobilized at the so-called connection moment. From here after the tether length remains constant. The evolution of the deployed tether is followed in order to record the specific behavior when the length of the tether is extremely great. The motion of the two connected masses and of the mass center proves completely non-Keplerian, beginning with the libration around local vertical due to the considerable residual kinetic moment at connection. A practical application of the quasi-vertical libration is in orbital passive debris collector, when a sandwich composite large panel is orbited for long periods of time for collecting small mass, high velocity Earth orbit debris. The most promising and controversial application of such long tethers resides in the anchoring technique to achieve the skeleton of a future space elevator. The stability of motion is an important aspect which is approached my numerical simulations.

Key-words: - Astrodynamics, Space tethers, Tether dynamics, Large space structures, Tether instability.

1 Introduction

Tether systems were first proposed as replacing means of the gas-dynamical propulsion systems for descent, landing and return from far celestial bodies, orbital transfer maneuvers, orbital launch from sub-orbital flight trajectories, entry into the atmosphere by space scoop devices and finally the anchoring of the presumed space elevator from orbit. Generally they are considered as potential substitutes of the costly and mass expensive conventional rocket propulsion systems. The phase of a free, un-powered deployment and the subsequent orbital evolving of tethered masses are under consideration. A series of published results are present in the open literature, as listed in the reference chapter, including those from the five International Conferences on Space Elevators (2001-2005), from the five International Conferences on Tethers in Space and recent presentations to the IAC dedicated sessions.

A lot of work was devoted to the study of the dynamics of large tethers, early researches showing that great challenges are related to the stability of such large systems [19], [21], [25], [26].

The relative reluctance towards tether systems can only be overcome when significant advantages from the use of space tethers, either for Earth orbital missions or for distant planetary missions, are proved. Regarding the orbital descent and ascent for example, the question is if tethers offer a better alternative to rocket propulsion and this could prove mainly important when deployment and anchoring to the Earth surface of a space elevator is considered.

The analysis here presented is based on the assumption that the technological problems related to ultra-long space cables are solved and now the problems of their exploitation in the space environment must be analyzed, prior to decide on the efficiency and specific design solutions.

The deployment phase is decisive for the dynamics of tethers. The technique here adopted is called the “free tether”, as far as friction-like or other kinematical restrictions on the deploying string are considered as negligible. The deployment starts by implementing a given, small impulse between the main orbital object and the tethered mass, or between equal tethered masses. The relative impulse is achieved by small size spring or pyrotechnical means. Consequently he masses are inserted into different orbits that end in a continuous departure between each-other, up to a convenient distance that will be eventually set constant at *connection* [2].

It is known that a continuous departure of the objects only occurs in the condition of a horizontal initial impulse, while a vertical separation induces repeated rejoining at each completed orbit. The eventual motion in free space must be observed by specific equipment that must continuously follow the line of sight between the departing masses, at ever increasing distances of the order of tens of kilometers and more. The attitude control during deployment is compulsory as the only means to guarantee a frictionless liberation of the required cable length during the departure of the two masses. In other words, the cable releasing system must predict the tether deployment under normal conditions and avoid any brake or friction loss during this essential phase of free deployment.

The next problem of connection is essentially a mater of mechanical collision, when the radial relative velocity is bluntly suppression at the connection moment. Some shock-type discontinuities in the motion of the tethered system intervene, absorbed in part by the elasticity of the system but tending to end in global tether system instability. A residual rotational momentum always persists and sends the system into the known “*dumbbell libration*” (Lorenzini [3]). The problem of minimizing the collision stresses in the cable is also a problem of optimal tether design and the numerical simulations play an important role. It is the scope of this research to demonstrate the possibilities of the proposed free deployment by numerical simulations.

Design of the attitude control system during deployment is essentially based on the prediction of the relative motion of the end-masses during this phase and the simulation must begin with this aspect. The amplitude of motion and the related overall characteristics of the optical/microwave transducers for line of sight control will result. The real design must also consider the large errors that might occur and must be properly balanced.

2 Prediction in the free deployment

The following assumptions are consistent:
- the gravity field is spherical, free of any non-symmetrical components;
- astronomical perturbations of the Moon and Sun are negligible;
- the orbiting masses are material points associated to their center of mass;
- the mass and weight of the tether string are negligible;
- the tether is flexible but inextensible;
- no time relaxation occurs.

Consequently, the elliptical motion of the splitting masses remains to be considered here, after the initial separation by the horizontal impulse (HIS). Prior to HIS, a circular satellite orbit is assumed for the non-deployed tether, with the connected objects moving at the constant altitude h_0 with the circular absolute velocity

$$w_0 = \sqrt{K_\oplus / r_0} \,. \tag{1}$$

Hereafter $K_\oplus$ denotes the gravity constant of the Earth with $K = fM$ in general.

At the HIS moment ($t = 0$) the velocity impulse Δw_0 is administered in the direction of flight and, denoting by $\mu = m/M$ the ratio of masses of the accelerated and decelerated objects respectively, the two bodies enter separate orbits with the insertion velocities

$$v_0 = w_0 + \frac{1}{1+\mu}\Delta w_0 \,, \qquad V_0 = w_0 - \frac{\mu}{1+\mu}\Delta w_0 \,. \tag{2}$$

The corresponding orbits (polar coordinates) of the accelerated and lower-orbiting masses respectively, behaving with eccentricities ε and E, are described by:

$$r = \frac{p}{1+\varepsilon\cos(\theta-\theta_0)} \,, \; R = \frac{P}{1+E\cos(\Theta-\Theta_0)} \,. \tag{3}$$

In the given circumstances the insertion point for the upper mass is located in its apoapsis and for the lower one in its periapsis. Assuming the common space-time origin at these specific points (θ_0 and $\Theta_0 = 0$, namely $r_P = R_A = r_0$) and using the kinematics of motion [7] and the vis-viva equation, the two orbits are described by

$$r = \frac{p}{1+\varepsilon\cos\theta} \,, \quad v^2 = K_\oplus\left(\frac{2}{r} - \frac{1}{a}\right), \tag{4}$$

$$R = \frac{P}{1-E\cos\Theta} \,, \quad V^2 = K_\oplus\left(\frac{2}{R} - \frac{1}{A}\right), \tag{5}$$

$$\mathbf{r} = \frac{p}{1+\varepsilon\cos\theta}\begin{bmatrix}\cos\theta\\ \sin\theta\end{bmatrix},\ \mathbf{v} = \sqrt{\frac{K_\oplus}{p}}\begin{bmatrix}-\sin\theta\\ e+\cos\theta\end{bmatrix}. \quad (6)$$

The velocity of the upper object m develops lower and the speed of the lower object M performs higher, with the orbital parameters

$$\varepsilon = r_0\frac{v_0^2}{K_\oplus} - 1,\ \ a = \frac{r_0}{1-\varepsilon},\ \ p = r_0(1+\varepsilon), \quad (7)$$

$$E = 1 + r_0\frac{V_0^2}{K_\oplus},\ \ A = \frac{r_0}{1+E},\ \ P = r_0(1-E). \quad (8)$$

On each orbit the speed **v** has a particular value and direction in space, depending on the position **r** on the orbit and given by [7]:

$$\mathbf{v} = \sqrt{\frac{K_\oplus}{p}}\cdot\frac{1+e\cos\varphi}{p}\begin{bmatrix}0 & -1\\ 1 & \dfrac{e}{\sin\varphi}\end{bmatrix}\cdot\mathbf{r}. \quad (9)$$

The relative distance d gradually increases, standing the mechanism of the *free tether deployment*. Note that the right anomaly is a cyclic coordinate. The Kepler local time is:

$$t = \frac{T_m}{2\pi}(\nu - \varepsilon\sin\nu),\ T_m = \frac{a}{v_0}\sqrt{\frac{1+\varepsilon}{1-\varepsilon}}, \quad (10)$$

$$t = \frac{T_M}{2\pi}(N + E\sin N),\ T_M = \frac{A}{V_0}\sqrt{\frac{1+E}{1-E}}. \quad (11)$$

The eccentric anomaly are ν and N for the upper m and lower M masses, while the corresponding periodic times are T_m and T_M. Time is measured from the common HIS origin, from the periapsis of mass m and apoapsis of M. These periodic times are

$$T_m = \frac{2\pi a^2\sqrt{1-\varepsilon^2}}{r_0 v_0},\ T_M = \frac{2\pi A^2\sqrt{1-E^2}}{r_0 v_0}. \quad (12)$$

The computational sequence for this twin-constellation flight is thus

$$Data \to t(common) \to \nu_1,\nu_2 \to \theta_1,\theta_2 \to \{x_1,y_1,x_2,y_2\}.$$

The Gauss substitution [2] transfers the eccentric anomalies into the true anomalies by the non-linear transforms:

$$tg\frac{\nu}{2} = \sqrt{\frac{1-\varepsilon}{1+\varepsilon}}\,tg\frac{\theta}{2},\quad tg\frac{N}{2} = \sqrt{\frac{1-E}{1+E}}\,tg\frac{\Theta}{2}. \quad (13)$$

These are the space references for eccentric and true anomalies and must be based on the eigen-periapsis of each orbit (3). They play the role of the primary referential in the present simulations, where the method of the running origin is finally used for visualization of the relative motion during deployment and further.

3 Free deployment phase

Although the constellation flight problem is direct, special precautions are mandatory. The correct positioning of time origin on each orbit is one. The Kepler equations (2) require a Newton-Raphson iterating solution for the eccentric anomaly at a common time value, although some other efficient numerical techniques are under development. Because the relative motion of the constellation bodies manifests extreme amplitudes, while the Earth-body distance remains always high, the numerical code can only be run in double precision. In the case of Fig. 1 the common duration of deployment is 2100 seconds and the common height angle is 34.9º, no matter how great the separation impulse Δw_0 is.

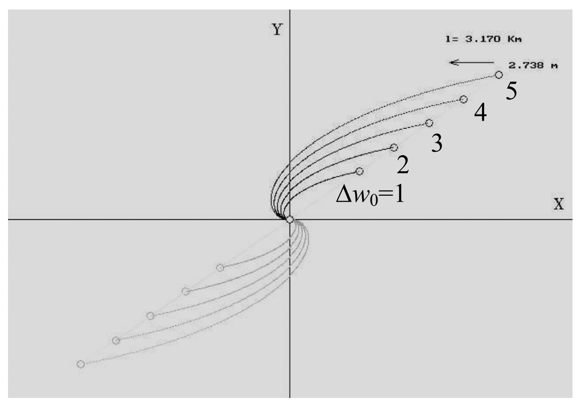

Fig.1: Free tether deployment for 2100 s.

The angular amplitude of the motion does not depend on the initial relative velocity and a outstanding similitude ot the family of trajectories results. At such a local scale the motion of the twin masses in respect to the starting pole O preserves almost symmetrical, where the components of the speeds are given by

$$\mathbf{v} = \dot{r}\boldsymbol{\rho} + r\dot{\theta}\boldsymbol{\tau},\qquad \mathbf{V} = \dot{R}\mathbf{R} + R\dot{\Theta}\mathbf{T},$$

$$\dot{d} = (r\dot{r} + R\dot{R} - (\dot{r}R + r\dot{R})\cos\delta + rR\dot{\delta}\sin\delta)/d \quad (14)$$

These are the entering values for the connection process of the orbital system, as the main parameters in the conservation lows which follow.

4 Tether connection

At the *connection point* (CP), meaning at the very moment when the planned tether length is attained and the tether free deployment is instantly blocked, during that short time interval the conservation laws of momentum and moment of momentum show that these parameters keep constant as far as internal forces are only present. Negligible small variations in the external forces occur and consequently one may describe the status of the momentum as:

$$\mathbf{H}_c - \mathbf{H}_e = \int \mathbf{F}\,\mathrm{d}t \approx \mathbf{F}\,\Delta t\,,\ \Delta t \to 0\,,\ \mathbf{H}_c = \mathbf{H}_e\,, \tag{15}$$

$$\mathbf{K}_c - \mathbf{K}_e = \int (\mathbf{r}\wedge\mathbf{f} + \mathbf{R}\wedge\mathbf{F})\,\mathrm{d}t \approx \mathbf{M}_\mathrm{F}\,\Delta t\,,$$
$$\Delta t \to 0\,,\ \mathbf{K}_c = \mathbf{K}_e\,. \tag{16}$$

While the kinetic moment, moment of momentum and the position of the masses are insignificantly altering, the speed components manifest drastic changes, similar to the variations encountered during collisions. The following relations (see also Fig.2) account for the conservation laws:

$$\begin{aligned}
\dot r_c &= \frac{K_{\mathrm{M}e}}{ml}\sin\psi + \frac{H_{le}}{1+\mu}\cos\psi\,,\\
r\dot\theta_c &= \frac{H_{le}}{1+\mu}\sin\psi - \frac{K_{\mathrm{M}e}}{ml}\cos\psi\,,\\
\dot R_c &= \frac{K_{\mathrm{m}e}}{Ml}\sin\Psi - \frac{H_{le}}{1+\mu}\cos\Psi\,,\\
R\dot\Theta_c &= -\frac{H_{le}}{1+\mu}\sin\Psi - \frac{K_{\mathrm{m}e}}{Ml}\cos\Psi\,,
\end{aligned} \tag{17}$$

The symbols used and the geometry of the tethered orbiters are shown in Fig. 2 and summarized on the next page.

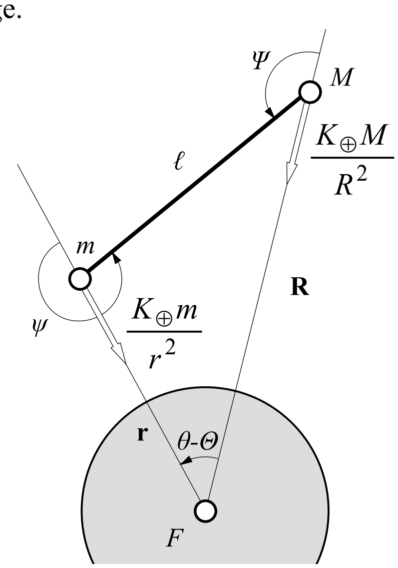

Fig.2: Tether geometry in a central field.

The set (17) of kinematical conditions assure the transfer from the preliminary free motion to the definite motion after stop of deployment. While writing the above formulae the notations were used

$$\begin{aligned}
H_{le} &= \mu(\dot r_e\cos\psi + r\dot\theta_e\sin\psi) - \dot R_e\cos\Psi - R\dot\Theta_e\sin\Psi,\\
\frac{K_{\mathrm{m}e}}{Ml} &= \dot R_e\sin\Psi - R\dot\Theta_e\cos\Psi,\\
\frac{K_{\mathrm{M}e}}{ml} &= \dot r_e\sin\psi - r\dot\theta_e\cos\psi.
\end{aligned} \tag{18}$$

The tether motion is eventually subjected to an important gravity gradient, visible due to the large scale of the tethered structure in respect to the radius of the central body. The behavior is highly nonlinear and this ends in a markedly non-Keplerian motion and even instability, as numerically proved below. No closed, analytical solutions for this motion are available [2], [4], [6], [20], [24], although a series of analytical analyses of the character of the motion were already performed [19], [21], [25], [26]. Numerical computations of the actual tether orbital evolution were much less emphasized and are here presented in detail, as performed by proprietary simulation codes [18].

5 Numerical simulation

The description of tether motion presents intrinsic difficulties[18], due to the inconvenient geometry, almost parallel directions of the position vectors and large variations in the angular reciprocal positions of the masses involved. The related computational instabilities were specifically solved. The 2-D problem is governed by 3 degrees of freedom, namely 3 dependent variables.

5.1 The differential equations

Consequently, the three second order differential equations have the following form (9) of ODE-s:

$$\begin{cases}
Q \equiv \left[\dfrac{K_\oplus}{\ell}\left(\dfrac{\cos\psi}{r^2} + \dfrac{\cos\Psi}{R^2}\right) + \omega^2\right],\\[2mm]
\ddot\theta = -2\dfrac{wu}{r} - \dfrac{R\sin(\theta-\Theta)}{(1+\mu)\,r}\cdot Q\,,\\[2mm]
\ddot\Theta = -2\dfrac{ZV}{R} + \dfrac{\mu\,r\sin(\theta-\Theta)}{(1+\mu)\,R}\cdot Q\,,\\[2mm]
\ddot r = r\,u^2 + \dfrac{R\cos(\theta-\Theta) - r}{1+\mu}\cdot Q - \dfrac{K_\oplus}{r^2}.
\end{cases} \tag{19}$$

The geometric relations follow the data in Fig.2:

$$\begin{cases} \ell\cos\psi = R\cos(\theta-\Theta) - r, \\ \ell\cos\Psi = r\cos(\theta-\Theta) - R, \\ \ell\sin\psi = -R\sin(\theta-\Theta), \\ \ell\sin\Psi = r\sin(\theta-\Theta), \\ \ell\omega^2 = \left(R\ddot{\Theta} + 2\dot{R}\dot{\Theta}\right)\sin\Psi + \left(\ddot{R} - R\dot{\Theta}^2\right)\cos\Psi + \\ \qquad + \left(r\ddot{\theta} + 2\dot{r}\dot{\theta}\right)\sin\psi + \left(\ddot{r} - r\dot{\theta}^2\right)\cos\psi. \end{cases} \tag{10}$$

In the Kane form, ready for numerical integration, the equations of motion read

$$\begin{cases} \dot{\theta} = f_\theta(u) \equiv u, \\ \dot{u} = f_u(\theta, \Theta, r, R, u, w), \\ \dot{\Theta} = f_\Theta(V) \equiv V, \\ \dot{V} = f_V(\theta, \Theta, r, R, V, Z), \\ \dot{r} = f_r(w) \equiv w, \\ \dot{w} = f_w(\theta, \Theta, r, R, u). \end{cases} \tag{11}$$

6 Numerical results

The Earth constants used all along are $K_\oplus$ =3.987624457·10^{14} m^3/s^2 for the gravity and $r_\oplus$ = 6371221 m for the Earth radius. A regular and apparently periodical gravity coupling appears for Lunar tethers with lengths comparable to the Lunar orbit (Fig. 3).

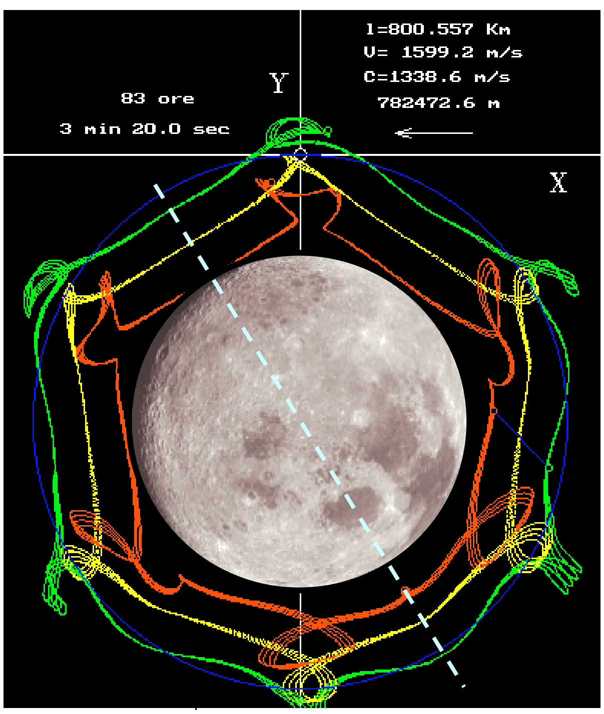

Fig. 3: Lunar gravity coupling.

Similar resonance manifests at least for satellite tethers of Europa and Rhea. Values of K_E =3.20419804·10^{12} m^3/s^2 and r_E =1561000 m are for Europa and K_R =1.542020305·10^{11} m^3/s^2 and r_R =764000 m for Rhea[10,11]. Decagonal geometry is observed as given in Fig. 4 for an orbit at 1000 km above Europa. For carefully implemented Speeds at HIS at different given altitudes of the orbit the periodicity of motion develops remarkable. A line of symmetry also appears, always inclined as referred to the HIS point on the circular initial orbit (the running origin in the draft).

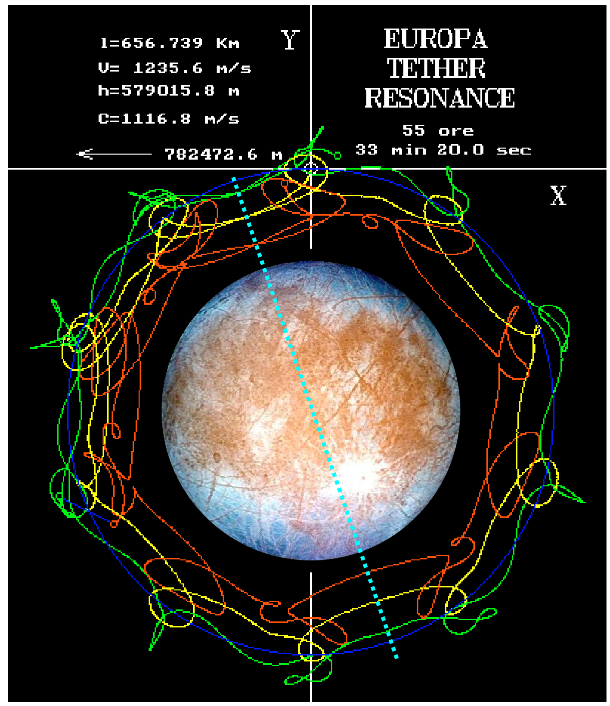

Fig. 4: Europan tether decagonal resonance.

A double-pentagonal configuration of resonance appears for a specific motion around Rhea (Fig. 5). The length of the tether system for this configuration represents 54% from the Saturnian satellite radius. To be more visible, this motion is drawn in figure 5 for the mass center of the tether (yellow line) only. The initial circular orbit is drawn in blue and the entire relative motion is again regarded to the running origin of the deployment on the circular initial orbit. Due to the curvature of the orbit, the momentum conservation of the system at connection produces a decrease in the kinetic energy and the eventual orbit of the structure always remains lower than the starting circular orbit. The initial conditions of the tether at connection asure a length of the cable of 416 km, while the Rhean radius is of 764 km. The cable length remains well below the radius of the central body.

The drop in kinetic energy is more visible for larger tethers and, as discussed by several authors, finally ends in a total instability of the motion, when the tether length becomes extremely great.

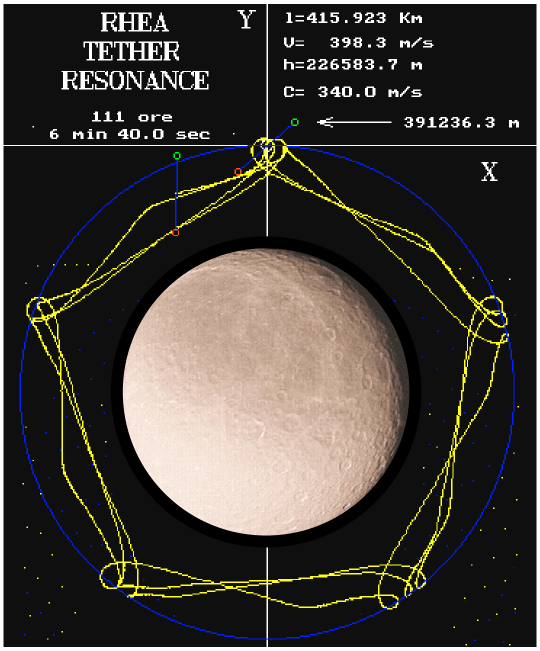

Fig. 5: Rhean double-pentagonal resonance.

Up to that point however, the motion of the system performs always below the circular orbit, as visible in all numerical simulations here presented. The problem of flying tether systems with length greater then the orbital radius is not physically possible, as it results in immediate crash of the lower mass on the planet surface.

7 Orbital instability

Previous analytical observations [19], [26] regarding the instability of motion for very long tethers, nearing the orbital radius, show that the tether motion is rather unstable. The condition is deduced that the unstable tether should be longer than its orbital radius (Troger [19]), but this condition is already practically impossible. They are confirmed by direct numerical computations. At the same time the observation must be made that structures with sizes comparable to the radius of the initial circular orbit are in fact impossible. Due to the residual negative amount of energy after connection, a tether system with the length equal to the altitude of the initial orbit will crash before even completing its first revolution around the body. As structures larger than the radius of the orbit are nonsense, the problem of the stability must be worked out for structure sizes smaller than the altitude of the circular orbit above the planet surface (Fig. 6).

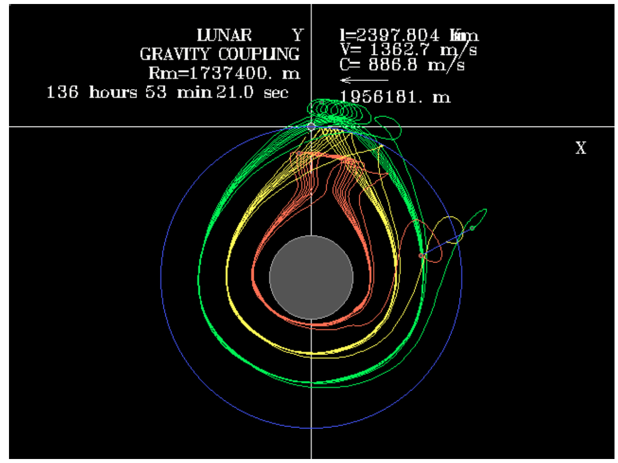

Fig. 6: Orbit instability for a large Lunar tether.

The initial circular orbit selected for this applications hovers at 4500 km above the Lunar surface, where a relative HIS velocity of 142.4584311 *m/s* is implemented between the two tethered masses. A deployment for 194 *minutes* produces a tether length of 2,397,804 *m*, much larger than the Lunar radius (1,737,400 *m*). During the first seven revolutions, the trajectories seem to perform stable and regular, each turn around the central body goes very near to the previous one, as seen in the draft 5. A small lag is recorded however and this accumulates to produce a rapid change into instability after revolution 8, ending in a crash during the 18th revolution. Changes as small as one $\mu m / s$ suffice to change the character of the motion, occurrence that also shows, after Liapunov's theory, the presence of an unstable region.

A relevant situation regarding the effect of very small changes in the initial conditions is also given in figure 7. For the same orbital altitude the HIS velocity is increased to 142.4584311 *m/s* and this produces a positive lag of the orbits, ending in a late crash after 27 orbits and 448 hours of evolution.

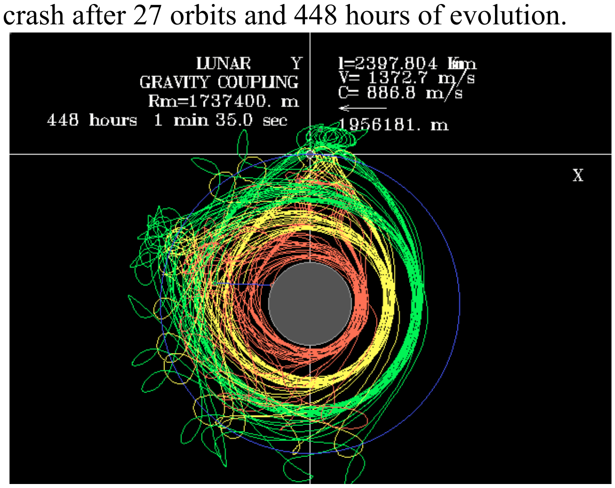

Fig. 7: Late instability for very large tethers.

The effect of the majestic gravity gradient is visible as far as the libration of the tether during the evolution on the lower part of the trajectory, very near to the Lunar surface, is completely suppressed. Here the effect of centrifugal forces within the tethered structure is overwhelming. The lower mass is fastly sweeping the Lunar surface with double of the circular velocity (1372.7 m/s) at an altitude of a few kilometers. It is once more obvious that the condition of a tether longer than the orbital altitude, to say nothing of more than the orbital radius, is impossible to consider. This criterion of Troger [19] or Beletsky [20] remains in fact purely theoretical.

8 Orbital stability after Scheeres

A lot of research is devoted to the so-called generalized two-bodies problem (GTBP), where the bodies engaged into reciprocal gravitational influence are no more replaceable by two mass points or particles. They manifest a visible size and irregular mass distribution in comparison to the distance between the two, coupled bodies. This induces important gravity gradient effects when the bodies are rigid or even tidal effects when they are elastic or fluid, with sensible energy dissipation and loss of stability. For the rigid body assumption the mechanical interaction ends into non-Keplerian effects and even high instability. Scheeres had shown that the condition of stability is that the whole mechanical energy be negative,

$$E(h, v, \omega) < 0 \tag{9}$$

and this condition should be proved by the present simulation also. The twin tether is in fact the extreme case of the non-spherical mass distribution, presenting the most elongated ellipsoid of inertia among all possible mass distributions achievable in practice. The non-Keplerian behavior and all other gravity gradient effects outlined in the theory of GTBP are thus maximal in this study case.

9 Conclusions

The ultra-large scale twin space tethers prove being the extreme cases of non-Keplerian celestial bodies, where the non-linear effects of the gravitational gradient are maximal. These effects are highly surpassing all possible situations for common planetary bodies like the small, very non-spherical asteroid systems, largely approached by recent studies. Consequently the tether systems play the role of a benchmark research tool in non-linear astrodynamics.

A lot of works had shown through theoretical investigations that for such systems the orbital motion could get unstable. The accurate numerical simulation of both equal and non-equal, twin-mass tether systems in LEO and around other bodies shows possible unpowered deployment scenarios with consequent stable librating motion of the system, when the connection between the two end-masses is settled in advance of the smooth point of connection and the tether length is smaller than the radius of the central body.

For time intervals below one sideral day little if any extinguish process was found on the oscillatory motion that performs regular and at least quasi-periodic. The entire study was performed under convenient, simplifying assumptions. The stability of the tethered masses was also accounted by calculating the variation of the force in the string. A stable configuration means a positive value of the tension. The librating motion proves almost always stable, while the tumbling rotation ends always in instability. This is a real challenge for tether landing, as repeated approach of the lunar soil is highly desirable for a safe landing.

Combinations of HIS velocities and altitudes are always found which provide conveniently stable motion, but this greatly depends on the initial conditions of flight and the type of deployment. A high precision of the maneuvers is required to assure the success of the landing. Tether evolution in case of ultra-high length of the cable is usually unstable, but offers support for a number of orbital evolutions in quasi-stable configuration. This is an important observation regarding landing projects by tethers.

College Station, on August 24, 2006.

References:

[1] D. A. Vallado, *Fundamentals of Astrodynamics and Applications*, Space Technology Series, The McGraw-Hill Companies, Inc., New York-Toronto, 2001;

[2] E. Messerschmid, S. Fasoulas, *Raumfahrtszsteme*, *Chap.4.6 Tethers im Gravitationsfeld*, Springer, 2000;

[3] E. C. Lorenzini, *Novel Tether-Connected Two-Dimensional Structures for Low Earth Orbits*, Journal of the Astronautical Sciences, **36**, 4(1988), pp. 389-405.

[4] M.L. Cosmo, E. Lorenzini, *Space Tehters Handbook*, NASA Marshall S.F.C. Grant NAG8-1160, 1997;

[5] Steven E. Patamia, *Space Elevator Transverse Oscillations with Free Boundary Conditions*, The Space Elevator: 2nd Annual International Conference, Santa Fe, New Mexico, September 12-15, 2003;

[6] J. Allyn Smith, C. Butler, *Deployment Scenarios*, The Space Elevator: 2nd Annual International Conference, Santa Fe, New Mexico, September 12-15, 2003;
[7] D. Mortari, "*On the Rigid Rotation Concept in n-Dimensional Spaces*" Journal of the Astronautical Sciences, Vol. 49, No. 3, July-September 2001;
[8] Forward, R. L., "Tether Transport from LEO to the Lunar Surface", AIAA Paper 91-2322, *27th Joint Propulsion Conference*, Sacramento, CA, June 1991;
[9] Hoyt, R.P., Forward, R. L., "Tether Transport from Sub-Earth-Orbit to the Moon... and Back!," *1997 Int. Space Development Conference*, Orlando Fl, May 1997;
[10] Hoyt, R.P., Uphoff, C.W., "Cislunar Tether Transport System", AIAA Paper 99-2690, 35th Joint Propulsion Conference, June 1999;
[11] *Guide to Planetary Satellites*, *Sky/Telescope*, 2004;
[12] Rothery D. *Satellites of the Outer Planets*, Clarendon Press, Oxford. 208 pp., 1992.
[13] R. D. Rugescu, C. Morosanu, *Debris Hazards Mitigation by Orbital Recovery*, Paper IAC-05-D4.P.04, 56th IAC, October 16-22, 2005, Fukuoka, Japan.
[14] http://www.iza-structure.org/databases/
[15] J.-C. Liou, M. Matney, P. Anz-Meador, D. Kessler, and J. Theall, "ORDEM2000's Debris Environment Model", *The Orbital Debris Quarterly News*, NASA Johnson Space Center, **6**, 1, January 2001, p.4.
[16] D. J. Kessler, "Tools for Rule-of-Thumb Calculations for Orbital Debris", *The Orbital Debris Quarterly News*, NASA Johnson S. C., **7**, 3(2002).
[17] Burt, R. and E.L. Christiansen, *Hypervelocity Impact Tests on Hubble Space Telescope (HST) Solar Array Cells*, JSC technical report 28307, May 2001.
[18] R. D. Rugescu, *Tethers as far mission descent-return tools*, 55th IAC, Paper IAC-04-IAA.3.8.2.04, Vancouver, Canada, October 2004.
[19] N. Pugno, H. Troger, A. Steindl, M. Schwarzbart, *On the Stability of the Track of the Space Elevator*, IAC-06-D4.2.05, 57th IAC, Valencia, Spain, 2-8 Oct. 2006.
[20] Beletsky, V. V., Levin, E.M., 'Dynamics of Space Tether Systems', Adv. Astronautical Sciences, 83, 1993.
[21] Simo, J. C., Lewis, D.,'Energy methods in the stability analysis of relative equilibria of Hamiltonian systems'. The Proceedings of the sixth Symposium on Continuum Models and Discrete Systems, Dijon, June 1989, 162– 183. Editor: G.A. Maugin. Longman.
[22] Marsden, J. E., Lectures on Mechanics, London Math. Soc., Lect. Notes 174, Cambridge U. Press, 1992.
[23] Marsden, J.E. and Ratiu, T. S., An Introduction to Mechanics and Symmetry, A Basic Exposition of Classical Mechanical Systems, Springer-Verlag, New York – Heidelberg – Berlin, 1994.
[24] Wang, L.-S., Chern, S.-J., Shih, C.-W., 'On the dynamics of a tethered satellite system', Archives for Rational Mechanics and Analysis, 127; 1994, 297-318.
[25] Krupa, M., Schagerl M., Steindl A., Szmolyan, P. and Troger, H., 'Relative equilibria of tethered satellite systems and their stability for very stiff tethers', Dynamical Systems **16**, 2001, pp. 253-287.
[26] M. Krupa1, M. Schagerl, A. Steindl, H. Troger, Stability of Relative Equilibria. Part I: Comparison of Four Methods, *Meccanica* 35: 325–351, 2001.
[27] Krupa, M., Steindl A., Troger, H., 'Stability of Relative Equilibria. Part II: Dumbell Satellites', Meccanica 35:353–371, 2001.
[28] R. P. Patera, Collision Probability for Larger Bodies Having Nonlinear Relative Motion, Journal of Guidance, Control and Dynamics, Vol. 29, No. 6, November–December 2006, pp. 1468-1471.
[29] Scheeres, D., Hsiao, F.-Y., Park, R., Villac, B., and Maruskin, J., "Fundamental Limits on Spacecraft Orbit Uncertainty and Distribution Propagation," AAS Paper 05-471, 2005.
[30] Martin, L., D. J. Scheeres, Stability Bounds for Three-Dimensional Motion Close to Asteroids, Journal of Astronautical Sciences, **50**, 4 (Oct.-Dec. 2002) p. 389.
[31] W. Hu, D. J. Scheeres, 'Numerical determination of stability regions for orbital motion in uniformly rotating second degree and order gravity fields', Planetary and Space Science 52 (2004), pp.685 – 692
[32] F.Y. Hsiao, D. J. Scheeres, 'Bifurcations and dynamical evolution of eigenvalues of Hamiltonian systems', Physica D 213 (2006), pp. 66–75.
[33] Ryan S. Park, Daniel J. Scheeres, 'Nonlinear Mapping of Gaussian Statistics: Theory and Applications to Spacecraft Trajectory Design', Journal of Guidance, Control and Dynamics, 29, 6 (2006), pp. 1367-1375.
[34] Junkins, J., Akella, M., and Alfriend, K., "Non-Gaussian Error Propagation in Orbit Mechanics", Journal of the Astronautical Sciences, **44**, 4(1996), pp. 541–563.
[35] Scheeres, D. J., Han, D., Hou, Y., "Influence of Unstable Manifolds on Orbit Uncertainty," Journal of Guidance, Control and Dynamics, **24**, 2001, pp. 573–585.
[36] Shen, Q., Tabarrok, B., 'Stability Investigation of Multibody Spacecraft', ZAMM, Z. Angew. Math. Mech. **79** (1999), 3, pp. 161-170.
[37] Kamman, J. W., and Huston, R. L., "Modeling of Variable Length Towed and Tethered Cable Systems," J. Guid. Contr. Dyn., **22**, 4(1999), pp. 602–608.
[38] Xiang Zhou, Junfeng Li, H. Baoyin, Vadim Zakirov, Equilibrium Control of Electrodynamic Tethered Satellite Systems in Inclined Orbits, Journal of Guidance, Control and Dynamics, Vol. 29, No. 6, 2006, pp. 1451–1454.